

Radar-Based Structural Monitoring of Wind Turbines Blades: Field Results from Two Operational Wind Turbines

MORITZ MÄLZER¹, SEBASTIAN BECK¹, SERCAN ALIPEK¹, ELIAS REICHART¹, JOCHEN MOLL¹, VIKTOR KROZER¹, CHRISTOS OIKONOMOPOULOS², JÜRGEN KASSNER², MANFRED HÄGELEN², THOMAS HEINECKE³, BURKHARD CERBE³, JONAS ROSE³, VESA KLUMPP⁴, MARTIN BERGER⁵ and MARIO KOHL⁵

ABSTRACT

Wind energy plays a prominent role in Germany to achieve the climate targets. According to the "Wind-an-Land-Gesetz" (literally: "Wind on Land Act"), which has just come into force, the area used for onshore wind energy in Germany should be more than doubled from the current 0.8% to 2% until 2032.

Rotor blades are one of the most significant cost factors of a wind turbine. They contribute with about 30% to the plant costs. By means of continuous monitoring of their structural integrity, it would be possible to reduce downtime and maintenance costs. This approach of "structural health monitoring" (SHM) with FMCW-radar systems has already been tested in the laboratory.

In this contribution, we describe and demonstrate an SHM system for radar-based monitoring of rotor blades at two operational wind turbines. For this purpose, a sensor box with a 35 GHz radar sensor (1 000 measurements per second) and a camera system (100 images per second), is mounted on each wind turbine tower at approximately 100 m height. In order to distinguish individual rotor blades, a machine-readable marker printed on a self-adhesive film was applied on the blade's surface. When a rotor blade passes the sensor, the camera captures an image of the marker while the radar records a measurement. The marker is then identified and the recorded data is assigned to a particular rotor blade. The ultimate goal is to detect damage-induced changes in the radar characteristic of the blades.

By end of April, over 260 000 rotor blade passes had already been recorded. The data set will be discussed in the paper. Images from the FMCW-radar are classified by the rotor blade label using a convolutional neural network (CNN). Early test results for a subset already show an f1-score of 0.886 and 0.923 for each rotor blade of the evaluated wind turbine.

¹Department of Physics, Goethe University of Frankfurt am Main, Frankfurt am Main, Germany, Email: moll@physik.uni-frankfurt.de

²IMST GmbH, Kamp-Lintfort, Germany

³cp.max Rotortechnik GmbH & Co. KG, Dresden, Germany

⁴Knowtion GmbH, Karlsruhe, Germany

⁵BOREAS Energie GmbH, Dresden, Germany

INTRODUCTION

Operation and maintenance accounts for 33.6% of the levelized cost of electricity for onshore wind projects on average over 25 years. This includes in particular the rotor blades, which account for around 30% of the capital expenditure (CapEx) of a wind turbine [1]. Currently, wind turbine rotors are mainly visually inspected for damage at regular intervals. Continuous monitoring using Structural Health Monitoring (SHM) techniques could allow maintenance intervals to be adjusted as needed, thus saving costs. In recent years, SHM using FMCW radar has been investigated for blade damage detection. It has already been demonstrated in the laboratory that damage can be detected using a 35 GHz FMCW radar [2]. Radar sensors can also be used for SHM applications in the 60 GHz band as demonstrated on coupon level [3] and during a recent full-scale fatigue test using a 31m long wind turbine blade [4].

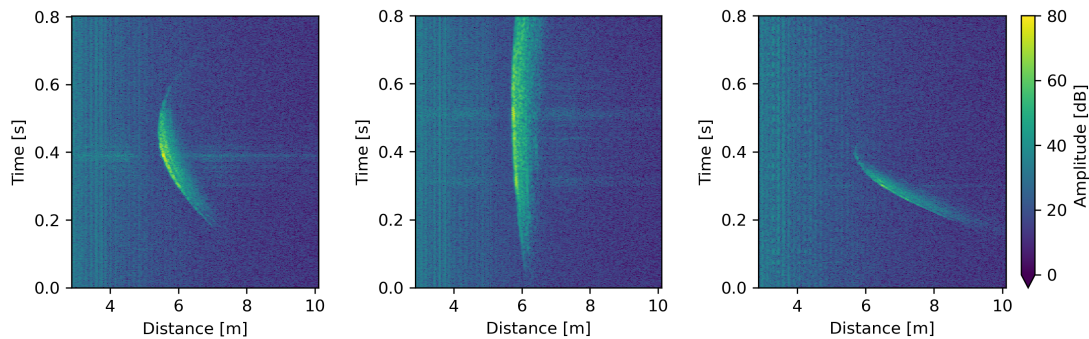
Since damage detection generally requires a reference measurement from intact structural conditions, it is necessary to know to which rotor blade a specific measurement belongs. It will be investigated whether it is possible to assign blades based on radar data alone, but the development of such algorithms requires the availability of labelled training data. To obtain this, machine-readable codes were applied to the rotor blades. Each time a rotor blade passes by, a camera records a short video. This allows each measurement to be assigned to a rotor blade. In addition to video and radar data, information from the turbine control system, such as wind direction, wind speed and blade pitch, is also recorded. These parameters have an influence on the radar measurement and can affect the comparability of a measurement with a reference. The possibility of eliminating the need to access the turbine control system in the future is being investigated. The ultimate goal of the research project is to develop a system that can detect damage based on the radar data and support future customers in their decision making. To this end, a new 35 GHz multichannel FMCW radar sensor has been developed. The use of multiple channels could also enable other functions besides damage detection, such as the detection of ice on rotor blades.

Recent works on structural health monitoring of wind turbines using deep learning methods focused on optical images of damaged rotor blades taken by UAVs for non-operating turbines. Applied convolutional neural networks (CNNs) range from regular image classifiers [5, 6] to bounding box detectors [7, 8] that locate potential areas of damage. Optical images give only information about the turbine blade surface and are highly sensitive to daylight exposure. The usage of UAVs usually limits the evaluation to non-operating turbines. Insights from this work provide a foundation for a reliable and automatic monitoring system for operating wind turbines with FMCW radar data.

The remainder of the paper is organized as follows: First, an overview of the measurement system and the measurement procedure is given. Subsequently, the data sets already gathered are explored and discussed. Based on this, first evaluation attempts for radar-based rotor blade discrimination are presented. Finally, the further outlook is presented.



Figure 1. The sensor unit on the tower (left) and a rotor blade with barcode (right top) and AI marker (right bottom).



(a) rotation speed: 6.2 rpm nacelle orientation: 247.9° (b) rotation speed: 1.8 rpm nacelle orientation: 225.0° (c) rotation speed: 13.0 rpm nacelle orientation: 267.3°

Figure 2. An overview of the radargrams of different rotor blade passes from the same wind turbine. A clear influence of the wind-turbine parameters can be seen. The color axis applies to all three radargrams.

STRUCTURE OF THE MEASURING SYSTEM

A measuring system will be mounted on each of three wind turbines at about 90 m height. As of early May 2023, two systems were already operational. Each measurement system consists of two different units, one mounted on the outside of the wind turbine tower and one unit inside the tower on a platform, as well as different markers on each rotor blade. The unit mounted outside the wind turbine is referred to as the *sensor unit*, and the unit mounted inside the wind turbine is referred to as the *supply unit*. Classical barcodes as well as markers for video-based AI-supported differentiation were applied to the rotor blades (see Figure 1).

The sensor unit consists of a box containing the radar sensor, a Raspberry Pi HQ camera, a Raspberry Pi 4B single board computer with an external SSD for data storage and a Power over Ethernet (PoE) splitter. The unit is mounted in such a way that the radar sensor covers the main wind direction. This ensures that the rotor blades are in view most of the time. The camera lens was chosen to cover a similar area.

A measurement is triggered by the radar using a threshold value. As soon as the radar detects a rotor blade in the detection area, the radar data (see Figure 2), as well as a short video and various metadata are automatically stored.

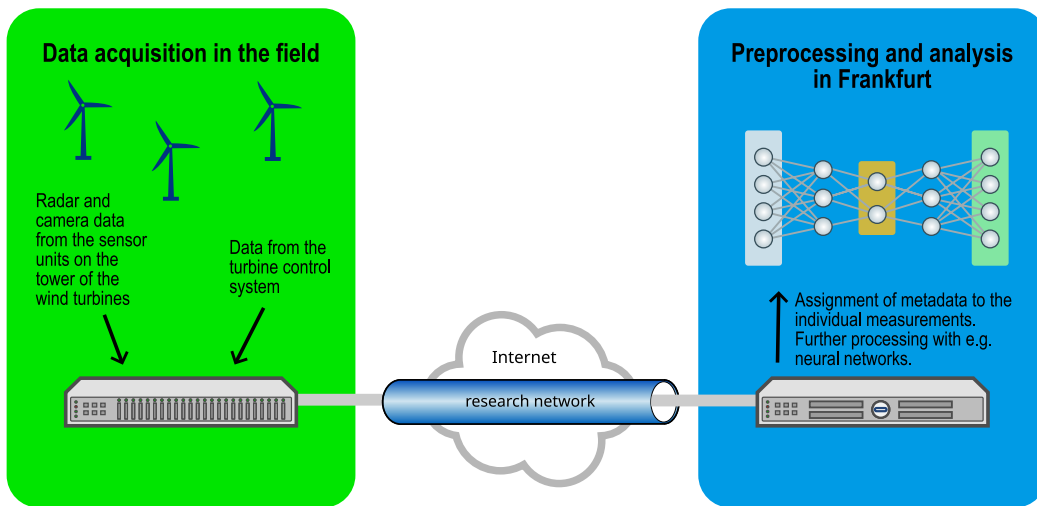


Figure 3. Data flow from the sensors to the server in Frankfurt.

The supply unit consists of a Raspberry Pi Zero single board computer which controls a relays. The relays controls the power supply of a PoE injector. The PoE injector delivers power and ethernet to the outer unit. The supply unit is connected to the wind farm network via a fiber optic cable leading to the tower base.

To collect data from all three systems, a computer is installed on site with access to the wind farms network and the research network used by Goethe University. This computer also receives data from the plant control system, such as wind speed or pitch angle of the rotor blades (see Figure 3).

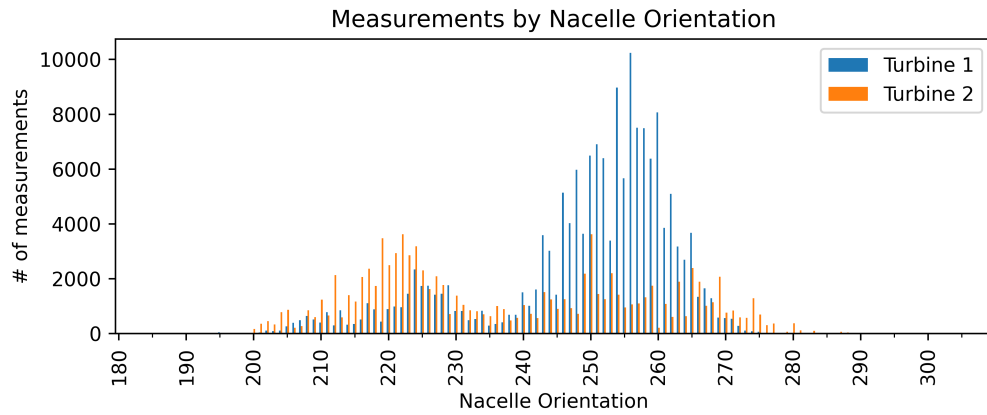
The collected data is then transferred as a whole to a server in Frankfurt, where some pre-processing steps are performed. These steps mainly include the assignment of the measurement to a particular rotor blade by means of barcode recognition. In addition, the measurements are merged with the corresponding data from the plant control system.

DATA SET AND PRELIMINARY ANALYSIS

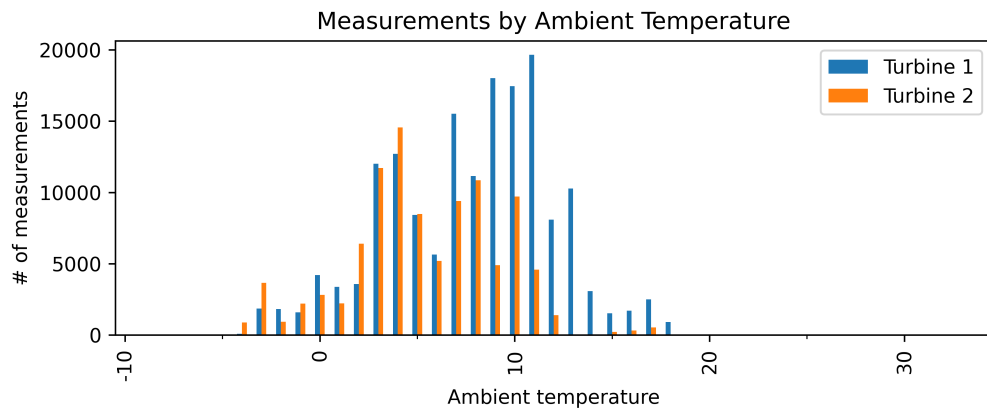
By the end of April 2023, more than 260 000 rotor blade passes had been recorded on the two turbines with the measurement system installed. In addition to the radar data (see Figure 2), a measurement consists of a video and various metadata. This includes the turbine control data and the settings with which the measurement system was operated.

The radar can detect the rotor blade for a nacelle orientation from 190° to 300° . This means a large azimuthal coverage of about 110° (see Figure 4a). The temperature range of the recorded data is from about -5°C to just below 20°C (see Figure 4b). The wind speeds in the data set range from no wind to over 25 m/s , although these speeds are rare and barely visible in the figure (see Figure 4c). The recorded measurements also cover the full range of the pitch angles that range from -6.7° to 47.6° with a few samples between 71° and 78° . Unfortunately, we do not have a precipitation sensor available, so this data would have to be obtained later from other sources if necessary.

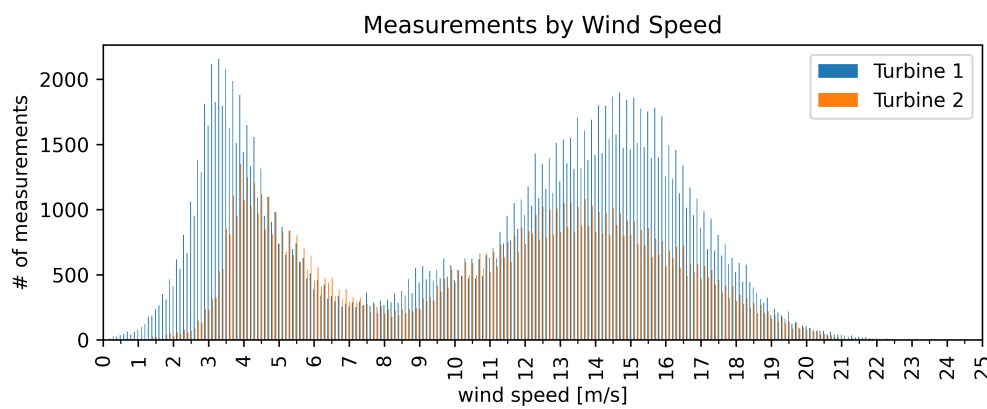
One sample contains a total of 44 metadata entries. Not all of these metadata are directly useful for analysis, some are only used to track possible errors. An example



(a) Histogram of measurements by nacelle orientation. Since it contributes to the angle of the rotor blade relative to the radar, it will have a significant impact on the radargram and thus on further analysis. Both radar systems are mounted at approx. 230°.



(b) Histogram of measurements by ambient temperature. The ambient temperature affects the rotor blade itself. Due to thermal expansion, the radar measurements differ at different temperatures.



(c) Histogram of measurements by wind speed. Wind speed is the main factor affecting the speed of the wind turbine. Thus, it determines how long the rotor blades are in front of the radar.

Figure 4. An overview over different metadata parameters.

TABLE I. RADAR-BASED ROTOR BLADE CLASSIFICATION.

Class	f1-score (train)	f1-score (val)	f1-score (test)
ROT1	0.987	0.920	0.911
ROT2	0.984	0.892	0.886
ROT3	0.987	0.918	0.923

would be the version of the measurement software. It is only stored to identify the affected part of the data set in case of a software malfunction.

It is also possible that some entries contain the same information or at least correlate. An example would be the nacelle orientation and the wind direction. In general, they should at least be similar. Therefore, it is necessary to find out which metadata is really relevant for the analysis.

RADAR-BASED ROTOR BLADE CLASSIFICATION

For the first test of a radar-based blade classification using a neural network, only a subset of the complete data set was used. In the period from October 21st, 2022 to March 31st, 2023, a total of 104 000 verified samples consisting of corresponding radargrams, labels and metadata were processed for turbine 1. For turbine 2, a total of 70 000 samples were extracted for the period from December 15, 2022 through February 25, 2023. The labels assigned by barcode recognition are assumed to be correct. This enables the application of supervised learning models. In the scope of this project, a simple convolutional neural network (CNN) was designed to classify a given rotor blade by a corresponding radargram. The CNN is defined by three consecutive convolution layers with intermediate batch normalization, rectified linear unit (ReLU) and max-pooling which are followed by two fully connected layers with an intermediate ReLU.

With the intention of reducing uncertainty in the model optimization, several metadata were integrated into the CNN. Included values are the outside temperature, wind speed, rotation speed of the turbine, pitch angle of the rotor blade, wind direction and nacelle orientation. The idea is to include only metadata that is likely to affect the measurement conditions, either by changing the sensor sensitivity or by changing the relative position and exposure of a rotor blade to the radar sensor. The angle value for wind direction and nacelle orientation is formatted into the coordinates of a point on the unit circle, resulting in a total set of eight metadata values assigned to the radargram and label of a given measurement. All metadata are normalized to intervals of $[0, 1]$ or $[-1, 1]$ for better interpretation by the CNN. The set of eight metadata values is then concatenated with the first fully connected layer (after the ReLU) and then connected with the last fully connected layer.

In the current stage of model development, a total of 11 500 valid samples collected between 03/20/2023 and 03/31/2023 were analyzed for turbine 1. The dataset was randomly partitioned into 6 900 training samples, 2 300 validation samples and 2 300 test samples. Metadata values were integrated as previously described. To evaluate the model performance, the f1-score was calculated as the harmonic mean of precision and recall. An overview of the scores after training the model for 10 epochs is shown in Table I. Class *ROTX* represents rotor blade number *X* of turbine 1. One can see that the training

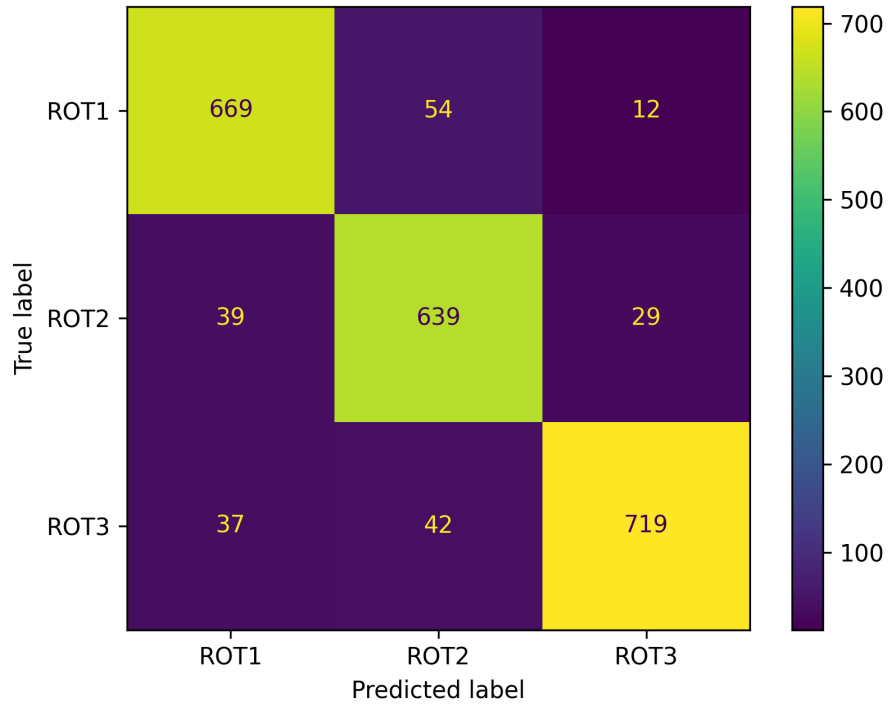


Figure 5. Confusion matrix of the optimized model applied on the test data of 2 300 samples in total.

data is almost fully comprehended by the CNN. The model shows a reduced classification score for the validation data and the test data unseen during optimization. The detection of *ROT2* inside a radargram is slightly worse compared to *ROT1* and *ROT3*. A closer look at the classification results is provided by the confusion matrix for the test set in Figure 5. With an f1-score of 0.984 to 0.987 for the training data, the model shows to comprehend the feature distribution of the training data. Applied on the validation data, seen during optimization and the test data, unseen during optimization, the model reaches an f1-score between 0.886 and 0.923.

The number of examples used only cover a small subset of the complexity of all features for each rotor blade. Such features are the characteristic reflection of a rotor blade combined with the relative position of the blade to the radar sensor paired with external (weather) conditions. Differences between individual rotor blades can be explained by manufacturing defects, minor differences in blade geometry or local thickness and density after manufacturing or by operational damages like erosion or hail. Taking that into account, a set of measurements, continuously collected across a year, should contain a reliable representation of common cases and features required for a robust and strong radar-based discrimination of rotor blades of a given turbine.

CONCLUSIONS AND OUTLOOK

In this paper we presented the setup of an SHM measurement system on two running wind turbines. An overview of the data sets was given and first analyses were performed using a CNN approach for rotor blade detection. The CNN shows good capabilities to distinguish the rotor blades based on the radar data alone.

First results on the radar-based classification of individual rotor blades, as shown in the previous section, indicate a promising future for the structural health monitoring of wind turbines and similar applications. The differences between individual blades are not visible to the naked eye in the radargrams. The same is true for minor damage. The fact that the former can be detected by a neural network makes us confident that damage can also be detected and possibly even classified.

ACKNOWLEDGMENT

The authors gratefully acknowledge the financial support of this research by the Federal Ministry for Economic Affairs and Climate Action (grant number: 03EE2035A).

REFERENCES

1. Stehly, T. and P. Duffy. “2020 Cost of Wind Energy Review,” Tech. rep., doi:10.2172/1838135.
2. Moll, J., P. Arnold, M. Mälzer, V. Krozer, D. Pozdniakov, R. Salman, S. Rediske, M. Scholz, H. Friedmann, and A. Nuber. 2018. “Radar-Based Structural Health Monitoring of Wind Turbine Blades: The Case of Damage Detection,” *Structural Health Monitoring*, 17(4):815–822, ISSN 1475-9217, 1741-3168, doi:10.1177/1475921717721447.
3. Moll, J., T. Maetz, M. Mälzer, V. Krozer, K. Mischke, S. Krause, O. Bagemiel, A. Nuber, S. Kremling, T. Kurin, F. Lurz, R. Weigel, and V. Issakov. 2021. “Radar-based Monitoring of Glass Fiber Reinforced Composites during Fatigue Testing,” *Structural Control and Health Monitoring*, 28(10), ISSN 1545-2255, 1545-2263, doi:10.1002/stc.2812.
4. Simon, J., T. Kurin, J. Moll, O. Bagemiel, R. Wedel, S. Krause, F. Lurz, A. Nuber, V. Issakov, and V. Krozer. 2023. “Embedded Radar Networks for Damage Detection in Wind Turbine Blades: Validation in a Full-Scale Fatigue Test,” *Structural Health Monitoring*:147592172311528, ISSN 1475-9217, 1741-3168, doi:10.1177/14759217231152815.
5. Yang, X., Y. Zhang, W. Lv, and D. Wang. 2021. “Image recognition of wind turbine blade damage based on a deep learning model with transfer learning and an ensemble learning classifier,” *Renewable Energy*, 163:386–397, ISSN 0960-1481, doi:https://doi.org/10.1016/j.renene.2020.08.125.
6. Reddy, A., V. Indragandhi, L. Ravi, and V. Subramaniaswamy. 2019. “Detection of Cracks and damage in wind turbine blades using artificial intelligence-based image analytics,” *Measurement*, 147:106823.
7. Mao, Y., S. Wang, D. Yu, and J. Zhao. 2021. “Automatic image detection of multi-type surface defects on wind turbine blades based on cascade deep learning network,” *Intelligent Data Analysis*, 25(2):463–482.
8. Qiu, Z., S. Wang, Z. Zeng, and D. Yu. 2019. “Automatic visual defects inspection of wind turbine blades via YOLO-based small object detection approach,” *Journal of electronic imaging*, 28(4):043023–043023.